

Time Delay Margin Analysis Applied to Model Reference Adaptive Control

Andrei Dorobantu*, Peter J. Seiler†, and Gary J. Balas‡,

Department of Aerospace Engineering & Mechanics

University of Minnesota, Minneapolis, MN, 55455, USA

Adaptive control has the potential to improve performance and reliability in aircraft. Implementation of adaptive control on commercial and military aircraft requires verification and validation of the control system's robustness to modeling error, uncertainty, and time delay. Currently, there is a lack of tools available to rigorously analyze the robustness of adaptive controllers due to their inherently nonlinear dynamics. This paper addresses the use of nonlinear robustness analysis for adaptive flight control systems. First, a model reference adaptive controller (MRAC) is derived for a linear aircraft short-period model. Sum-of-squares (SOS) polynomial optimization is applied to the closed-loop model to assess its robustness to time delay. Time delay margins are computed for various combinations of design parameters in the adaptive law, as well as in the presence of model uncertainty. This paper extends and refines previous work through the implementation of more advanced polynomial optimization algorithms and analysis conditions.

I. Introduction

Adaptive control has the potential to improve performance and reliability in aircraft. However, typical adaptive control architectures are inherently nonlinear. There is a lack of tools available to rigorously analyze the robustness and performance of such systems. The inability to verify robustness and performance is a significant roadblock to the implementation of adaptive control on civilian and military aircraft.

The primary objective of this paper is to demonstrate the suitability of sum-of-squares (SOS) polynomial optimization for the analysis of adaptive flight control systems. There has recently been significant research on SOS optimization problems, which have been used to analyze the performance and robustness of systems described by polynomial dynamics.¹⁻³ Computational algorithms have been developed for estimating regions of attraction, reachability sets, input-output gains, robustness with respect to uncertainty, and time delay margins.⁴⁻²⁰ Moreover, there is freely available software to solve SOS optimizations.²¹⁻²³

This paper demonstrates that SOS optimization can be applied to assess the robustness of adaptive flight control systems to time delay. An important and meaningful robustness metric is the time delay margin. SOS optimization is used to calculate lower bounds on this robustness metric, and Monte Carlo simulations are used to calculate upper bounds. This approach was previously applied to a flight control system with model reference adaptive control (MRAC).^{24,25} This paper extends the work in References 24 and 25 by refining the optimization algorithms and analysis.

An MRAC is derived for the linear short-period dynamics of an aircraft in Section II. Section III outlines the SOS optimization for time delayed systems, and formulates a time delayed version of the closed-loop MRAC system. Section IV summarizes the results of the time delay margin analysis, and Section V provides concluding remarks.

*Graduate Student, AIAA Student Member

†Senior Research Associate, AIAA Member

‡Professor, AIAA Associate Fellow

II. Aircraft Model and Controller

This section describes a linear aircraft model implemented with a model reference adaptive controller. Both the aircraft model and the controller are taken from Reference 26. This particular closed-loop system has been previously studied and analyzed for robustness using various techniques.²⁴⁻²⁶

A. Short-Period Aircraft Model

The X-15 was an experimental hypersonic rocket propelled aircraft flown in the 1960s. A short-period model of its longitudinal dynamics is given by Equation 1.

$$\begin{aligned}\dot{x} &= A_\lambda x + Bu \\ y &= Cx\end{aligned}\tag{1}$$

The states of the system are angle-of-attack α and pitch rate q , given by $x = [\alpha \text{ (deg)}, q \text{ (deg/sec)}]^T$. The input to the system is elevator deflection $u = \delta_{elev}$ (deg), and the output is the angle-of-attack $y = \alpha$ (deg). The subscript λ on the state matrix A_λ denotes parametric uncertainty. The state, input, and output matrices for the X-15 short-period model are defined in Equations 2 - 4.

$$A_\lambda = \begin{bmatrix} -0.2950 & 1.0000 \\ -13.0798\lambda_\alpha & -0.2084\lambda_q \end{bmatrix}\tag{2}$$

$$B = \begin{bmatrix} 0 \\ -9.4725 \end{bmatrix}\tag{3}$$

$$C = \begin{bmatrix} 1 & 0 \end{bmatrix}\tag{4}$$

The aircraft model is denoted P_λ , indicating that it is an uncertain system. The terms λ_α and λ_q model parametric uncertainty in two aerodynamic coefficients.²⁷ Defining an appropriate parameter space for the uncertainty is required for analysis. 75 % parametric uncertainty is considered by allowing the λ terms to vary on the interval $[.25 \ 1.75]$. The short-period dynamics remain stable throughout this uncertainty envelope.

The nominal state matrix is denoted A_{nom} and corresponds to $\lambda_\alpha = \lambda_q = 1$. Eigenvalue decomposition reveals that the nominal short-period mode has a damping ratio $\zeta = 0.07$ at a frequency $\omega_n = 3.63$ rad/sec. Hence, the short-period dynamics are lightly damped. One of the goals of the control design is to attenuate the oscillations corresponding to this mode.

B. Model Reference Adaptive Control

A model reference adaptive controller is applied to the X-15 short-period model. The MRAC is nonlinear and has four main components: a reference model, an adaptive law, and two constant gains. The closed-loop system interconnection is shown in Figure 1.

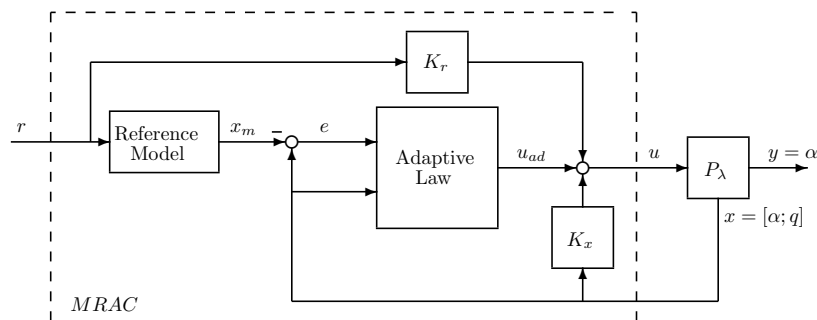


Figure 1. System interconnection for aircraft model with MRAC.

The interconnection shows that the control signal u is a summation of three signals. These signals originate from the state feedback gain K_x , the reference feedforward gain K_r , and the Adaptive Law. The resulting control signal u is the input to the aircraft model P_λ . Accordingly, the control law is defined by Equation 5.

$$u(t) = K_x x(t) + K_r r(t) + u_{ad}(t) \quad (5)$$

The state feedback gain K_x is designed first. Its objective is stability augmentation to increase damping in the short-period mode of the nominal model. The controller is designed using the LQR method with only the aircraft states, and minimizes the cost function J in Equation 6.

$$J = \int x(t)^T R_1 x(t) + u(t)^T R_2 u(t) dt \quad (6)$$

For the cost function J , the parameter weights R_1 and R_2 are selected as I_2 and 1, respectively. The resulting matrix K_x is shown in Equation 7.

$$K_x = \begin{bmatrix} 0.0577 & 0.9843 \end{bmatrix} \quad (7)$$

The inner-loop created by the stability augmentation system is overdamped with eigenvalues at -2.14 and -7.69. The inner-loop transfer function $G_{il}(s)$ is given by Equation 8.

$$G_{il}(s) = C [sI_2 - (A_{nom} + BK_x)]^{-1} B \quad (8)$$

The feedforward gain K_r is designed such that the output y tracks the input r at low frequency, and is defined with Equation 9.

$$K_r = G_{il}^{-1}(0) = [-C(A_{nom} + BK_x)^{-1} B]^{-1} = -1.7354 \quad (9)$$

Finally, the control signal u is augmented with u_{ad} , which corresponds to the adaptive law. This is the central feature of the controller. The adaptive law is defined in Equation 10.

$$u_{ad}(t) = \theta^T(t)x(t) \quad (10)$$

In this relationship, θ is a vector of adaptation parameters. The adaptation parameters are states of a virtual dynamic system, called the parameter update law and is defined in Equation 11.

$$\dot{\theta}(t) = -\kappa x(t)e^T(t)PB - \sigma\theta(t) \quad (11)$$

The error signal e is defined as the difference between the aircraft state x and the reference model state x_m . The reference model is equivalent to the nominal aircraft model in feedback with K_x and with K_r as a feedforward gain. In other words, the reference model is the transfer function $G_{il}(s)K_r$. The structure of the reference model is given in Equation 12.

$$\begin{aligned} \dot{x}_m &= (A_{nom} + BK_x)x_m + BK_r r \\ &:= A_m x_m + B_m r \\ y_m &= Cx_m \end{aligned} \quad (12)$$

Signal e is a characterization of the uncertain aircraft model's deviation from the nominal model. This deviation is the main driver in the parameter update law. If the aircraft model has no uncertainty, x and x_m are identically equal to each other. In this case, θ decays as a function of time since the error is zero. Hence, adaptation is driven by uncertainty in the aircraft model.

There are two tuning parameters in the parameter update law. κ is the adaptation gain, and σ is the sigma modification gain. The adaptation gain determines how quickly the θ dynamics evolve. The sigma modification gain adds robustness to the system by ensuring boundedness of the θ parameters. In this paper, κ and σ are varied and robustness of the closed-loop is examined.

The symmetric matrix variable P is also a control design parameter. It is calculated by solving the Lyapunov equation $A_m^T P + P A_m = -Q$, where $Q = 2I_2$. The Lyapunov function $V = x^T P x$ can be used to prove stability for the MRAC closed-loop system when $\sigma = 0$. Further, Barbalat's lemma can show

convergence of e to the origin. However, this analysis is no longer possible with the introduction of sigma modification. The value of P used in the control design is shown in Equation 13.

$$P = \begin{bmatrix} 1.8136 & 0.0341 \\ 0.0341 & 0.1085 \end{bmatrix} \quad (13)$$

The resulting closed-loop MRAC system is nonlinear. The adaptation parameters estimate uncertainty in the aircraft model, and feedback is used to drive the closed-loop dynamics towards the nominal condition. It is crucial to note that the closed-loop dynamics are polynomial, which is a requirement for SOS optimization. The only nonlinearities appear in the adaptive law and in the parameter update law. The closed-loop state equations are summarized by Equations 14 through 16.

$$\dot{x} = (A_\lambda + BK_x)x + B\theta^T x + BK_r r \quad (14)$$

$$\dot{x}_m = A_m x_m + B_m r \quad (15)$$

$$\dot{\theta} = -\kappa x(x - x_m)^T PB - \sigma \theta \quad (16)$$

The following section is focused on developing an approach that can be used to verify the robustness of this closed-loop system to time delay.

III. Time Delay Margin Analysis

An approach to calculating time delay margins for polynomial systems using SOS optimization was proposed in Reference 19, and refined in Reference 20. The approach in Reference 19 was used to analyze the MRAC system in References 24 and 25. This paper applies the refined approach in Reference 20 to improve the time delay margin results for the MRAC system.

In this section, a set of Lyapunov stability conditions is derived. These conditions can be used to prove stability of nonlinear systems with time delay. The conditions are subsequently relaxed, which allows them to be verified numerically via SOS optimization. Finally, the MRAC closed-loop dynamics are formulated as a time delayed system, which can be analyzed for robustness with SOS optimization.

A. Stability Analysis for Nonlinear Time Delayed Systems

A set of Lyapunov stability conditions is derived to prove stability of nonlinear systems with time delay. These conditions can be used to calculate a lower bound on the time delay margin. For the subsequent analysis, time delayed closed-loop dynamics are restricted to the form in Equation 17.

$$\dot{x}(t) = f(x(t), x(t - r)) \quad (17)$$

In this model, $x(t)$ is the current state vector, $x(t - r)$ is the delayed state vector, and the origin is an equilibrium point. Implicitly, this system is infinite dimensional. The current derivative depends explicitly on the current state and the delayed state. However, knowledge of the entire state time history on the time delay interval is required for predicting future states. This infinite dimensional time history is denoted ϕ_t , where $\phi_t \in [t - r, t]$. Many real systems can be modeled this way, such as systems with controller computation, communication, or transport delay. The largest r for which the equilibrium is stable is the time delay margin. The largest r for which stability can be numerically certified is a lower bound on that margin.

A Lyapunov function candidate is proposed in Equation 18, which maps the infinite dimensional vector ϕ_t into a real number.

$$V(\phi_t) = V_0(x(t)) + \int_{-r}^0 V_1(\tau, x(t), x(t + \tau)) d\tau + \int_{-r}^0 \int_{t+\tau}^t V_2(x(\xi)) d\xi, d\tau \quad (18)$$

$V(\phi_t)$ must be positive definite to guarantee stability. Positive definiteness of each term is sufficient but not necessary. Given at least one positive definite term, the others can be positive semidefinite. V_0 is constrained to be positive definite by ensuring that it is greater than the function $\psi = x(t)^T x(t)$. This allows for slack in the remaining terms. The kernels of the integral terms are constrained to be positive semidefinite. Indeed, the integral of a positive semidefinite function is positive semidefinite itself.

The time derivative \dot{V} must also be negative semidefinite to ensure stability. The manipulations required to simplify the form of this derivative are described in References 24 and 25. The simplified form is shown in Equation 19. The kernel of this integral is constrained to be negative semidefinite to certify stability of the time delayed system.

$$\begin{aligned} \frac{d}{dt}V = & \int_{-r}^0 \frac{1}{r} \frac{dV_o}{dx(t)} f + \frac{1}{r} V_1(0, x(t), x(t)) - \frac{1}{r} V_1(-r, x(t), x(t-r)) \\ & + \frac{\partial V_1}{\partial x(t)} f - \frac{\partial V_1}{\partial \tau} + V_2(x(t)) - V_2(x(t+\tau)) d\tau \end{aligned} \quad (19)$$

A set of sufficient conditions that prove local stability of the time delayed system in Equation 17 is formulated in Lemma 1.

Lemma 1 *Assume the origin is an equilibrium point for the system in Equation 17, functions V_0 , V_1 , and V_2 exist, and that $\psi(x(t))$ is a positive definite function such that:*

- 1) $V_0(x(t)) - \psi(x(t)) \geq 0$
- 2) $V_1(\tau, x(t), x(t+\tau)) \geq 0 \quad \forall \tau \in [-r, 0]$
- 3) $V_2(x(\xi)) \geq 0$
- 4) $\frac{1}{r} \frac{dV_o}{dx(t)} f + \frac{1}{r} V_1(0, x(t), x(t)) - \frac{1}{r} V_1(-r, x(t), x(t-r)) + \frac{\partial V_1}{\partial x(t)} f - \frac{\partial V_1}{\partial \tau} + V_2(x(t)) - V_2(x(t+\tau)) \leq 0 \quad \forall \tau \in [-r, 0]$

then the origin is a locally stable equilibrium for time delays up to size r .

The stability conditions in Lemma 1 apply to general nonlinear systems with time delay. With several assumptions and constraint relaxations, SOS optimization can be used to construct the Lyapunov function and certify the stability conditions. The next subsection details these assumptions and the constraint relaxation.

B. SOS Stability Analysis for Polynomial Time Delayed Systems

SOS optimization is limited to constraints on polynomial functions. Hence, the general nonlinear structure of the Lyapunov stability conditions described above cannot be implemented directly. However, if the system dynamics are limited to polynomials and the constraints are relaxed to SOS constraints, SOS optimization can be used to construct the Lyapunov function and certify the stability conditions. SOS analysis can thus be used to calculate a lower bound on the time delay margin for the system.

Conditions 2 and 4 in Lemma 1 are required to be positive definite on the interval $\tau \in [-r, 0]$. The interval restriction is not a polynomial object, hence it cannot be implemented as an SOS constraint. To remedy this, the constraints are relaxed using a variant of the S-procedure. A special polynomial function $h(\tau) = \tau(\tau+r)$ is defined. This function is negative semidefinite on the interval $\tau \in [-r, 0]$, and positive definite elsewhere. The function $h(\tau)$ is augmented to the conditions with SOS multiplier functions p_1 and p_2 , respectively. The resulting conditions are SOS constraints.

Similarly, the S-procedure is used to limit stability certification to a local region in the closed-loop system state space around the origin. This local region is described with a multidimensional box. Limiting certification to inside this box implies that there exists a local region of attraction. In particular, the largest level set of the Lyapunov function fully contained in the box is an invariant set. Hence, every trajectory originating from that level set is stable.

The magnitude of the box is defined by $|x_i| \leq \zeta_i$. Each x_i represents an individual state, and to allow flexibility, each direction is constrained independently in terms of ζ_i . Special polynomial functions similar in structure to $h(\tau)$ are defined. They are negative semidefinite in the local region, and positive definite elsewhere. Since $x(t)$, $x(t+\tau)$, and $x(t-r)$ are treated as separate sets of state variables in the optimization, three sets of h_{ji} functions are defined. Each state variable set is denoted with the j index. The i index is reserved for the individual state in a particular variable set. Consider the structure of h_{ji} functions shown in Equations 20 - 22. These h_{ji} polynomial functions augment the constraints on V_0 and on the kernel of \dot{V}

with their respective SOS multiplier functions q_{ji} .

$$h_{1i} = (x_i(t) - \zeta_i) (x_i(t) + \zeta_i) \quad (20)$$

$$h_{2i} = (x_i(t + \tau) - \zeta_i) (x_i(t + \tau) + \zeta_i) \quad (21)$$

$$h_{3i} = (x_i(t - r) - \zeta_i) (x_i(t - r) + \zeta_i) \quad (22)$$

Finally, Conditions 2 and 4 are augmented with polynomial functions r_1 and r_2 , respectively. These functions are used to improve the numerics of the optimization. To ensure that the Lyapunov stability conditions remain valid, equality constraints are enforced on the integrals of r_1 and r_2 . These equality constraints are shown in Equation 23.

$$\int_{-r}^0 r_1(x(t), \tau) d\tau = \int_{-r}^0 r_2(x(t), x(t-r), \tau) d\tau = 0 \quad (23)$$

The resulting stability conditions are complicated algebraically, but can be verified with an SOS program. In this paper, the Matlab toolbox SOSOPT is used for the optimization along with SeDuMi.^{23,28} SOS conditions for local stability of polynomial systems with time delay up to size r are summarized in Lemma 2.

Lemma 2 *Assume the origin is an equilibrium point for a polynomial system of the form in Equation 17, polynomial functions V_0 , V_1 , and V_2 exist, and that $\psi(x(t))$, p_i , q_{ji} , and r_i are positive definite polynomials such that:*

- 1) $V_0(x(t)) - \psi(x(t)) + \sum_{i=1}^n q_{1i} h_{1i}$ is SOS
- 2) $V_1(\tau, x(t), x(t + \tau)) + p_1 h(\tau) + r_1$ is SOS
- 3) $V_2(x(\xi))$ is SOS
- 4) $-r \frac{\partial V_1}{\partial x(t)} f - \frac{dV_0}{dx(t)} f + r \frac{\partial V_1}{\partial \tau} - r V_2(x(t)) + r V_2(x(t + \tau)) - V_1(0, x(t), x(t)) + V_1(-r, x(t), x(t - r)) + p_2 h(\tau) + \sum_{i=1}^n (q_{1i} h_{1i} + q_{2i} h_{2i} + q_{3i} h_{3i}) + r_2$ is SOS
- 5) $\int_{-r}^0 r_1(x(t), \tau) = 0$
- 6) $\int_{-r}^0 r_2(x(t), x(t - r), \tau) = 0$

then the origin is a locally stable equilibrium for time delays up to size r .

The SOS conditions in Lemma 2 can be directly implemented as an SOS program. The conditions certify that all trajectories originating from the largest level set of the Lyapunov function contained in the local box are stable for all time delays up to size r . The remaining task is to formulate the MRAC closed-loop dynamics as a time delayed polynomial system.

C. Time Delayed MRAC Closed-Loop Dynamics

A pure time delay of magnitude r seconds is introduced in the closed-loop system dynamics between the controller and aircraft model. This time delay can be interpreted physically as a computation, sampling, or network delay. A single time delay is considered in the dynamics for simplicity.

The SOS conditions derived previously apply to systems of the form in 17. A key point is that the polynomial closed-loop system must be autonomous. Hence, the input signal r in the MRAC closed-loop system is neglected to satisfy this condition. Neglecting the input signal may appear limiting for a nonlinear system, since the choice of input and its size can generally lead to degradation of stability margins. In the case of the MRAC system, however, analysis with the particular input choice $r = 0$ still leads to insightful results. If the autonomous system does not have sufficiently large stability margins, the time-varying system cannot meet robustness requirements either.

The absence of the input signal r alters the MRAC system dynamics. The effect of the feedforward gain K_r is completely eliminated. The reference model state x_m is also zero for all time. This implies that the error signal e is always equivalent to the true aircraft state x , which alters the parameter update law. The

parameter update law in the absence of the reference signal is shown in Equation 24. Note that the adaptive term is governed by the quadratic term xx^T , instead of xe^T .

$$\dot{\theta} = -\kappa xx^T PB - \sigma \theta \quad (24)$$

The simplified system dynamics are represented by an updated interconnection shown in Figure 2. Although the system dynamics are different from the original MRAC, the new dynamics remain polynomial. Hence, the robustness of the closed-loop system can be analyzed with the proposed SOS optimization.

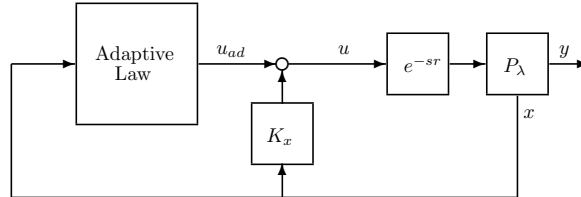


Figure 2. Simplified system interconnection neglecting input reference signal.

The SOS optimization certifies a set of local stability conditions for a box centered at the origin in the MRAC closed-loop system state space. Simulations of the nominal, undelayed system are used to guide the definition of this box in the locally stable region. For the controller design, adaptation gain and sigma modification values of 1 are used. Simulations are initialized with the state $[\theta_1(0), \theta_2(0), \alpha(0), q(0)]^T = [0, 0, \alpha_o, q_o]^T$, where α_o and q_o are sampled along a rectangle centered on the origin in $\alpha - q$ space. The results from simulations show that the locally stable region is at least ± 2 deg on α and ± 5 deg/sec on q . The locally stable region in the adaptation parameter space is at least ± 0.8 and ± 1.4 in θ_1 and θ_2 . Together, four state space constraints form a four-dimensional box that is fully contained in the undelayed nonlinear system locally stable region.

SOS optimization constructs a Lyapunov function that is valid inside the box in the MRAC closed-loop system state space. However, this does not prove that the entire box is a locally stable region. It is only guaranteed that V is positive definite, and that \dot{V} is negative semidefinite in the box. The guaranteed locally stable region is characterized by the largest level set fully contained in the box, and for time delays up to size r .

IV. Results

The SOS optimization is used to find a lower bound for the time delay margin. Monte Carlo simulations provide an upper bound. Since the exact margin is unknown, both the upper and lower bounds are needed for analysis. The SOS lower bound is meaningful if it lies above a required minimum value of time delay margin. In this case, the lower bound certifies that the flight control system meets the time delay margin requirement. Conversely, the Monte Carlo upper bound is meaningful if it falls below the requirement. In this case, the upper bound demonstrates that the time delay margin requirement is not satisfied. It cannot be determined if the minimum time delay margin is satisfied if the bounds straddle the requirement. In this case, however, the bounds can provide qualitative insight into trends in the time delay margin evaluated over a certain parameter space.

A reasonable minimum time delay margin requirement for the MRAC closed-loop system can be inferred from the open-loop aircraft model. The open-loop bandwidth is 5.6 rad/sec. A typical performance and robustness phase margin requirement at the system bandwidth is 45 deg.²⁹ At 5.6 rad/sec, this requirement translates to a time delay margin of about 140 msec. Thus, a reasonable minimum time delay margin requirement for the MRAC closed-loop system is also 140 msec.

The parameter update law in the MRAC is tuned by adjusting adaptation rate and sigma modification. Tuning the parameter update law determines the adaptive contribution to the MRAC control signal. If the adaptive component is turned off, the MRAC becomes a linear system. Hence, the full closed-loop system is linear, and a precise time delay margin can be calculated. This time delay margin is calculated using the loop transfer function $L(s) = K_x P(s)$, in which the aircraft model is assumed to be nominal. With adaptation turned off, the time delay margin for the system is around 151 msec. This calculated margin exceeds the minimum requirement of 140 msec.

The calculation of time delay margin is desired for the MRAC closed-loop system with active adaptation. Trends in the time delay margin are found due to variations in the MRAC tuning parameters as well as for uncertainty in the aircraft model. The time delay margin results are interpreted in terms of trends in the upper and lower bounds, and the satisfaction of the minimum time delay margin requirement.

Sub-section A focuses on the effect of varying adaptation rate. In this analysis, sigma modification is held constant to isolate the effect of changing adaptation rate. Sub-section B focuses on the effect of varying sigma modification. In this analysis, adaptation rate is held constant to isolate the effect of changing sigma modification. The effect of uncertainty in the aircraft model is examined. Changes in the aircraft dynamics are analyzed, and time delay margins are calculated over the uncertainty parameter space. Sub-section D describes some of the limitations of SOS optimizations due to heavy computational requirements.

A. Adaptation Rate

Effects of varying adaptation rate on the robustness of the MRAC closed-loop system is explored by investigating time delay margin. The sigma modification term is constant at 1 for this analysis. An upper bound for the time delay margin is calculated using Monte Carlo simulations. In this process, random initial conditions are sampled in the local region for increasing values of time delay. The upper bound is found with the lowest time delay that results in a divergent trajectory. The lower bound is calculated with SOS optimization. Time delay margin trends due to variations in adaptation rate are summarized in Figure 3.

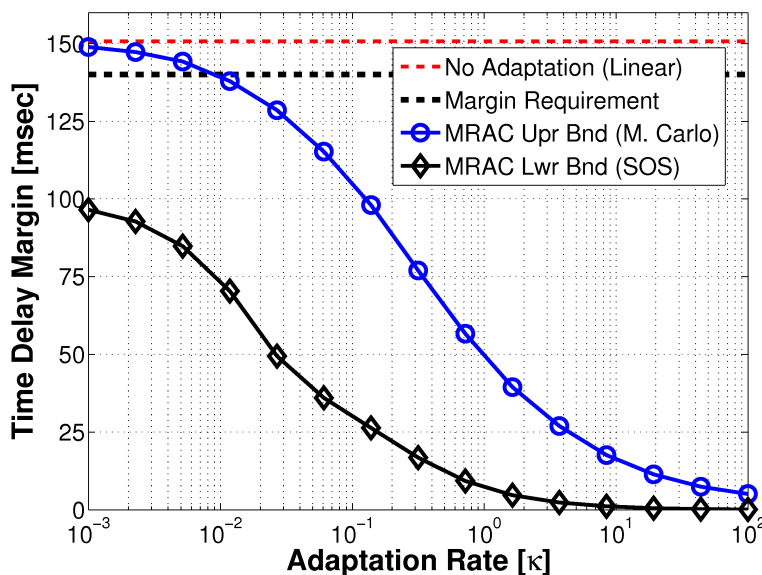


Figure 3. Time delay margin bounds as functions of adaptation rate.

The upper bound results confirm that decreasing κ leads to the convergence of the closed-loop MRAC system to the linear inner-loop. This result is intuitive as decreasing κ turns off the adaptive law. For higher adaptation gains, the upper bound decreases. This result is also intuitive as higher bandwidth in controllers leads to a decrease in robustness to time delay. For values of κ higher than 0.01, the minimum time delay margin requirement of 140 msec is no longer satisfied.

The lower bound exhibits the same trend as the upper bound. The gap between the bounds is significant for low adaptation rates. However, the trend in the true time delay margin is obvious. Together, the upper and lower bounds show that the time delay margin is highly sensitive to changes in the adaptation rate when $\kappa \in [0.01, 10]$. This is a region of interest because the adaptive law has influence over the aircraft dynamics on this interval.²⁵ Although the MRAC does not satisfy the robustness requirements in the region of interest for adaptation rate, the relationship between adaptation rate and time delay margin is revealed. Such insight cannot be drawn without the existence of a lower bound.

B. Sigma Modification

Time delay margin upper and lower bounds are calculated for varying sigma modification values. An adaptation rate of $\kappa = 1$ is held constant. The results in Figure 4 summarize the effect of varying sigma modification on the lower and upper bounds of time delay margin.

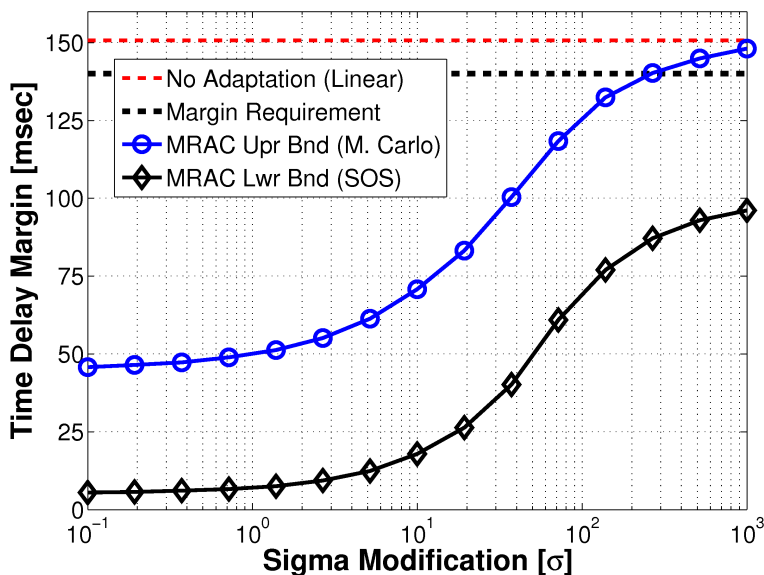


Figure 4. Time delay margin bounds as functions of sigma modification.

The upper bound in Figure 4 suggests that robustness to time delay increases with sigma modification. Further, it shows that the closed-loop system converges to the inner-loop for values above 1000. At this value, the adaptation is effectively turned off. It is impossible to design an MRAC that meets the robustness requirement with sigma modification less than 300. However, selecting such a high value greatly reduces the benefits of adaptation.

The lower bound results exhibit a similar increasing trend to the upper bound. There is a constant 40 msec gap between the bounds as sigma modification varies. For values of sigma modification below 1, the lower bound is constant at 7 msec. The bound shows a steep increasing trend for values between 10 and 100, and levels out beyond 1000 at around 100 msec. The lower bound is not able to show that the minimum time delay margin robustness requirement is met for any value of sigma modification. However, it provides evidence that sigma modification cannot increase robustness without sacrificing performance in the adaptation.

The bounds in Figure 4 provide significant insight into the qualitative trend of the true time delay margin despite the lower bound being conservative. The bounds imply that the time delay margin is constant for very low and very high values of sigma modification. They also indicate the range of values for which the time delay margin is most sensitive to changes in sigma modification. Knowledge of such sensitivities is crucial in control design. This type of insight cannot be drawn from the upper bound alone since it does not provide any analytically rigorous results. However, in conjunction with a guaranteed lower bound, the qualitative trends can be interpreted with more confidence.

C. Aircraft Model Uncertainty

The use of adaptive control is motivated by the need to account for uncertainty in the aircraft model without sacrificing performance. The goal of MRAC is to ensure nominal aircraft performance in the presence of variations in the system dynamics. Uncertainty is represented through the λ scaling parameters in the state matrix of the aircraft model. Each parameter varies on the interval $[0.25, 1.75]$ to encompass 75% uncertainty. A family of inner-loop transfer functions from elevator input to angle-of-attack output is calculated for this interval by sampling the parameter space. Figure 5 shows the frequency response of this family of transfer functions to illustrate the effect of uncertainty on the aircraft dynamics.

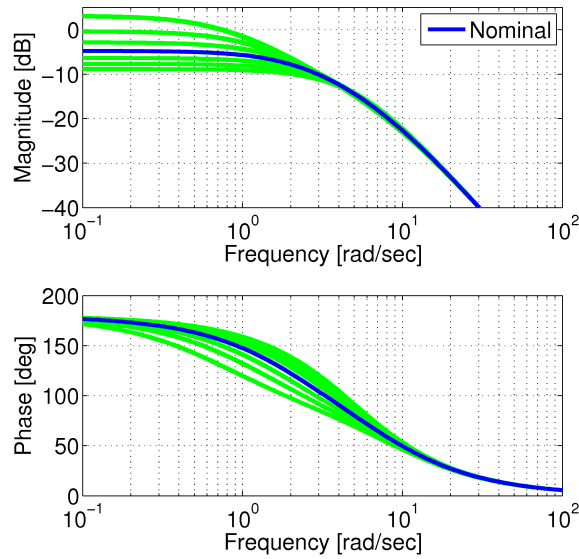


Figure 5. Inner-loop frequency response illustrating aircraft model uncertainty.

The results in Figure 5 suggest that uncertainty in the aircraft model is limited to changes in the low frequency characteristics of the inner-loop system. The nominal model is highlighted with the darker line on the plot. Deviations alter the DC gain of the system. The bandwidth of the system varies slightly, but this fluctuation does not affect the high frequency asymptote. This implies that the modes of the system do not vary independently due to uncertainty.

The dynamics of the closed-loop MRAC system are more sensitive to changes in λ_α than in λ_q . In the interest of computation time, λ_q is held fixed at its nominal value for this analysis. Time delay margins are calculated in the presence of 75 % uncertainty on λ_α to gain insight into its effect on robustness. An adaptation rate of 1 and a sigma modification value of 1 are selected for the adaptive law, supplying robustness without sacrificing performance in adaptation. Upper and lower bounds on the time delay margin are calculated with Monte Carlo simulations and SOS optimization, respectively. The results are summarized in Figure 6.

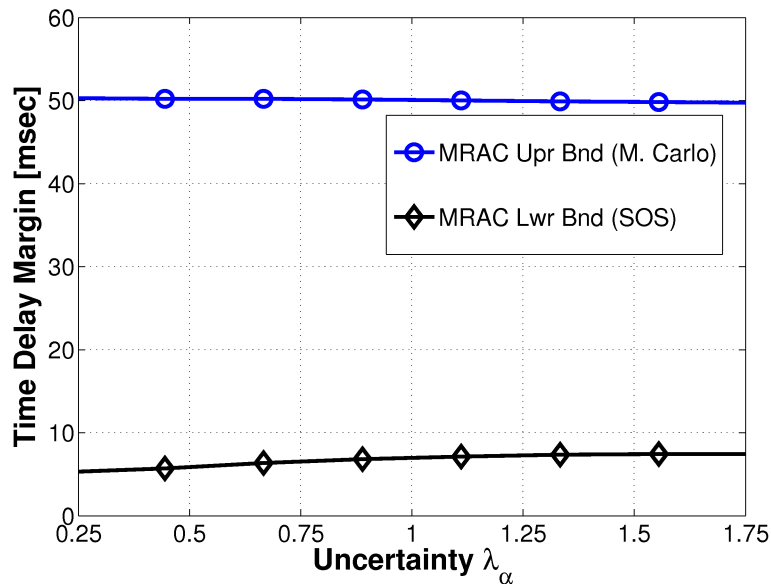


Figure 6. Time delay margin bounds as functions of aircraft model uncertainty.

The upper bound shown in Figure 6 shows that time delay margin is not sensitive to changes in the aircraft model due to parametric uncertainty. The lower bound is significantly more conservative, but confirms the same trend in the lack of sensitivity.

D. Limitations

A major limitation of the SOS optimization for calculating time delay margin is a shortage of memory and computation time. Roughly, the bisection required for each data point takes 20 minutes on a quad-core processor. Due to the structure of the Lyapunov function, the variable dimension of the system of equations that must be analyzed is three times the original system's dynamic order. Two extra sets of state variables are required to handle time delay, resulting in a total of 12 states. Due to the high state order, the Lyapunov function is limited to a second order polynomial. The computational load grows with the state order of the model. As such, computers run out of memory when attempting to solve time delay MRAC problems with quartic Lyapunov functions.

V. Conclusions

Adaptive control algorithms have the potential to improve performance and robustness in aerospace systems. However, there is a lack of tools available to rigorously analyze the robustness of these systems. This paper uses polynomial optimization tools to demonstrate the suitability of such analysis in the verification of adaptive control systems. The robustness of a model reference adaptive controller for a short-period aircraft model is examined in the presence of time delay. The sum-of-squares results are conservative, however, they are useful for gaining insight into trends in time delay margin due to variations in the control law and aircraft model.

Acknowledgments

This research was partially supported under the NASA Langley NRA contract NNH077ZEA001N entitled "Analytical Validation Tools for Safety Critical Systems" and the NASA Langley NRA Contract NNX08AC65A entitled "Fault Diagnosis, Prognosis and Reliable Flight Envelope Assessment." The technical contract monitors are Dr. Christine Belcastro and Dr. Suresh Joshi respectively.

References

- ¹Parrilo, P., *Structured Semidefinite Programs and Semialgebraic Geometry Methods in Robustness and Optimization*, Ph.D. thesis, California Institute of Technology, 2000.
- ²Lasserre, J., "Global Optimization with Polynomials and the Problem of Moments," *SIAM Journal on Optimization*, Vol. 11, No. 3, 2001, pp. 796–817.
- ³Parrilo, P., "Semidefinite programming relaxations for semialgebraic problems," *Mathematical Programming Ser. B*, 2003.
- ⁴Tibken, B., "Estimation of the domain of attraction for polynomial systems via LMIs," *Proceedings of the IEEE Conference on Decision and Control*, 2000, pp. 3860–3864.
- ⁵Hachicho, O. and Tibken, B., "Estimating domains of attraction of a class of nonlinear dynamical systems with LMI methods based on the theory of moments," *Proceedings of the IEEE Conference on Decision and Control*, 2002, pp. 3150–3155.
- ⁶Jarvis-Wloszek, Z., *Lyapunov Based Analysis and Controller Synthesis for Polynomial Systems using Sum-of-Squares Optimization*, Ph.D. thesis, University of California, Berkeley, 2003.
- ⁷Jarvis-Wloszek, Z., Feeley, R., Tan, W., Sun, K., and Packard, A., "Some Controls Applications of Sum of Squares Programming," *Proceedings of the 42nd IEEE Conference on Decision and Control*, Vol. 5, 2003, pp. 4676–4681.
- ⁸Papachristodoulou, A., *Scalable analysis of nonlinear systems using convex optimization*, Ph.D. thesis, California Institute of Technology, 2005.
- ⁹Jarvis-Wloszek, Z., Feeley, R., Tan, W., Sun, K., and Packard, A., *Positive Polynomials in Control*, Vol. 312 of *Lecture Notes in Control and Information Sciences*, chap. Controls Applications of Sum of Squares Programming, Springer-Verlag, 2005, pp. 3–22.
- ¹⁰Chesi, G., Garulli, A., Tesi, A., and Vicino, A., "LMI-based computation of optimal quadratic Lyapunov functions for odd polynomial systems," *International Journal of Robust and Nonlinear Control*, Vol. 15, 2005, pp. 35–49.
- ¹¹Prajna, S., *Optimization-Based Methods for Nonlinear and Hybrid Systems Verification*, Ph.D. thesis, California Institute of Technology, 2005.
- ¹²Tan, W., Packard, A., and Wheeler, T., "Local gain analysis of nonlinear systems," *Proceedings of the American Control Conference*, pp. 92–96.

- ¹³Tan, W., *Nonlinear Control Analysis and Synthesis using Sum-of-Squares Programming*, Ph.D. thesis, University of California, Berkeley, 2006.
- ¹⁴Tibken, B. and Fan, Y., “Computing the domain of attraction for polynomial systems via BMI optimization methods,” *Proceedings of the American Control Conference*, 2006, pp. 117–122.
- ¹⁵Tan, W., Topcu, U., Seiler, P., Balas, G., and Packard, A., “Simulation-aided Reachability and Local Gain Analysis for Nonlinear Dynamical Systems,” *Proceedings of the IEEE Conference on Decision and Control*, 2008, pp. 4097–4102.
- ¹⁶Topcu, U., Packard, A., and Seiler, P., “Local stability analysis using simulations and sum-of-squares programming,” *Automatica*, Vol. 44, No. 10, 2008, pp. 2669–2675.
- ¹⁷Topcu, U., *Quantitative Local Analysis of Nonlinear Systems*, Ph.D. thesis, University of California, Berkeley, 2008.
- ¹⁸Topcu, U. and Packard, A., “Linearized analysis versus optimization-based nonlinear analysis for nonlinear systems,” *Proceedings of the American Control Conference*, 2009.
- ¹⁹Papachristodoulou, A., “Analysis of Nonlinear Time-Delay Systems using Sum of Squares Decomposition,” *Proceedings of the American Control Conference*, 2004, pp. 4153–4158.
- ²⁰Papachristodoulou, A., Peet, M., and Lall, S., “Analysis of Polynomial Systems With Time Delays via Sum of Squares Decomposition,” *IEEE Transactions on Automatic Control*, Vol. 54, No. 5, 2009.
- ²¹Prajna, S., Papachristodoulou, A., Seiler, P., and Parrilo, P. A., *SOSTOOLS: Sum of squares optimization toolbox for MATLAB*, 2004.
- ²²Lofberg, J., “YALMIP : A Toolbox for Modeling and Optimization in MATLAB,” *Proceedings of the CACSD Conference*, Taipei, Taiwan, 2004.
- ²³Balas, G., Packard, A., Seiler, P., and Topcu, U., “Robustness Analysis of Nonlinear Systems,” <http://aem.umn.edu/~AerospaceControl/>.
- ²⁴Dorobantu, A., Seiler, P., and Balas, G., “Nonlinear Analysis of Adaptive Flight Control Laws,” *AIAA Guidance, Navigation, and Control Conference*, No. AIAA 2010-8043, 2010.
- ²⁵Dorobantu, A., *Time Delay Margin Analysis for Adaptive Flight Control Laws*, Master’s thesis, University of Minnesota, 2010.
- ²⁶Annaswamy, A., Jang, J., and Lavretsky, E., “Stability margins for adaptive controllers in the presence of time delay,” *AIAA Guidance, Navigation, and Control Conference*, No. AIAA 2008-6659, 2008.
- ²⁷Skogestad, S. and Postlethwaite, I., *Multivariable Feedback Control*, John Wiley and Sons Ltd., 2007.
- ²⁸Sturm, J., “SeDuMi version 1.05,” <http://fewcal.kub.nl/sturm/software/sedumi.html>, 2001.
- ²⁹Ogata, K., *Modern Control Engineering*, Prentice Hall, 4th ed., 2002.